JACS
JOURNAL OF THE AMERICAN CHEMICAL SOCIETY
Communication
pubs.acs.org/JACS

Growing Zigzag (16,0) Carbon Nanotubes with Structure-Defined Catalysts

Feng Yang,[†] Xiao Wang,[†] Daqi Zhang,[†] Kuo Qi,[‡] Juan Yang,[†] Zhi Xu,[‡] Meihui Li,[†] Xiulan Zhao,[†] Xuedong Bai,[‡] and Yan Li*,[†]

[†]Beijing National Laboratory for Molecular Science, Key Laboratory for the Physics and Chemistry of Nanodevices, State Key Laboratory of Rare Earth Materials Chemistry and Applications, College of Chemistry and Molecular Engineering, Peking University, Beijing 100871, China

[‡]Institute of Physics, Chinese Academy of Sciences, Beijing 100190, China

Supporting Information

ABSTRACT: The growth of zigzag single-walled carbon nanotubes (SWNTs) is most challenging among all types of SWNTs, with the highest reported selectivity of ~7%. Here we realized the dominant growth of (16,0) tubes at the abundance near ~80% by using intermetallic W_6Co_7 catalysts containing plenty of (1 1 6) planes together with optimizing the growth conditions. These (1 1 6) planes may act as the structure templates for (16,0) SWNTs due to the geometrical match between the open end of the (16,0) tube and the atomic arrangements of the (1 1 6) planes in W_6Co_7. Using catalysts with designed structure as solid state template at suitable kinetic conditions offers a strategy for selective growth of zigzag SWNTs.

The chirality selective growth of single-walled carbon nanotubes[1] (SWNTs) has long been a hot topic and also a great challenge in the field,[2−14] strongly related to their chiral index-dependent band structure.[15−18] Among all types of SWNTs, (*n*,0) type (zigzag) SWNTs are of special interest because of their symmetric structure and the difficulties in preparation.[19−25] It is found that the abundance of tubes with different (*n*,*m*) increases with increasing chiral angles in some bulk SWNT samples and that the (*n*,0) tubes are often undetectable.[21] Ding et al. recently showed by density functional theory (DFT) calculations that the growth rate of zigzag (*n*,0) SWNTs is significantly lower than that of other SWNTs.[25] Up to date, the highest population of zigzag SWNTs ever reported in the as-grown samples is ~7% of (13,0) tubes using cobalt catalyst pretreated with NH_3.[26] It is obvious that the selective growth of zigzag tubes is more challenging than other types of SWNTs. The unfavorable growth kinetics, which has been revealed by theoretical studies, is the main hurdle for achieving the preferable growth of zigzag tubes.

From the intensive efforts in the past 20 years, researchers begin to realize that epitaxial growth might be a possible strategy to control the chirality of the SWNTs. Both purified single chirality SWNT segments[27] and end-caps of the targeted SWNTs obtained from molecular precursors[28] have been used as the seeds and structural templates to grow SWNTs of specific chirality. If the efficiency could be improved, such processes would be very promising. Catalysts can also be used as the templates for epitaxial growth of SWNTs,[29,30] if the catalysts present a unique well-defined crystal structure. We used tungsten-based alloy, or more specifically, intermetallic compound W_6Co_7, as catalysts and synthesized (12,6) SWNTs with the purity higher than 92%.[31] The catalyzed SWNT growth is normally very efficient.

Epitaxial process enables the growth of a specific (*n*,*m*) type of SWNTs and remarkably limits the growth of tubes with other chiralities. Employing such strategy, the kinetic restriction in growing zigzag SWNTs may be resolved. Therefore, we tried to use W_6Co_7, which has unique crystal structure, to act as the catalyst template for the growth of zigzag tubes. In this attempt, first we need to prepare catalyst nanocrystals presenting the specific plane that matches the end structure of a zigzag tube.

We used the same tungsten−cobalt molecular cluster (denoted as $\{W_{39}Co_6O_x\}$) precursor, but performed the reduction process at 1050 °C, which is 20 °C higher than our previous study,[31] to prepare W−Co nanoparticles. As shown in Figures 1a and S1, the X-ray diffraction (XRD) pattern of the

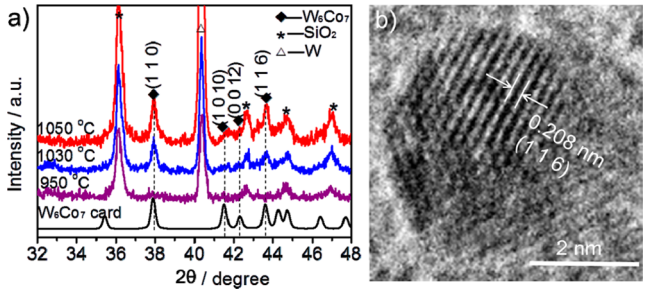

Figure 1. Characterizations of catalysts. (a) XRD patterns obtained on the fresh reduced catalysts at 950, 1030, and 1050 °C, respectively. Standard card of W_6Co_7 alloy from the database is also shown. (b) HRTEM image of a catalyst nanoparticle prepared at 1050 °C.

SiO_2-supported sample reduced at 1050 °C exhibits diffraction peaks fully ascribed to W_6Co_7, W, and SiO_2, respectively, which is similar to that obtained at 1030 °C. However, by normalizing the XRD patterns with respect to the intensity of (1 1 0) diffraction of W_6Co_7, it is found that the sample prepared at 1050 °C shows obviously a stronger (1 1 6) peak (appearing at 43.6°) than that

Received: April 28, 2015
Published: June 30, 2015

DOI: 10.1021/jacs.5b04403
J. Am. Chem. Soc. 2015, 137, 8688−8691

prepared at 1030 °C. This indicates that the population of (1 1 6) planes is evidently increased at 1050 °C. The high-resolution transmission electron microscopy (HRTEM) image exhibits lattice fringes with the intervals of 0.208 nm, which is in good accordance with the (1 1 6) plane distance of W_6Co_7 (Figure 1b).

We chose the catalyst structure cutting from the (1 1 6) plane of W_6Co_7 to study the structural match of SWNTs with different chiralities on the catalyst. The DFT simulations reveal that only the (16,0) SWNT among all the studied chiralities fits best to the atomic arrangements of (1 1 6) plane of the W_6Co_7 nanocrystal (Figures 2a–e and S2). Figure 2h shows that the interface energy,

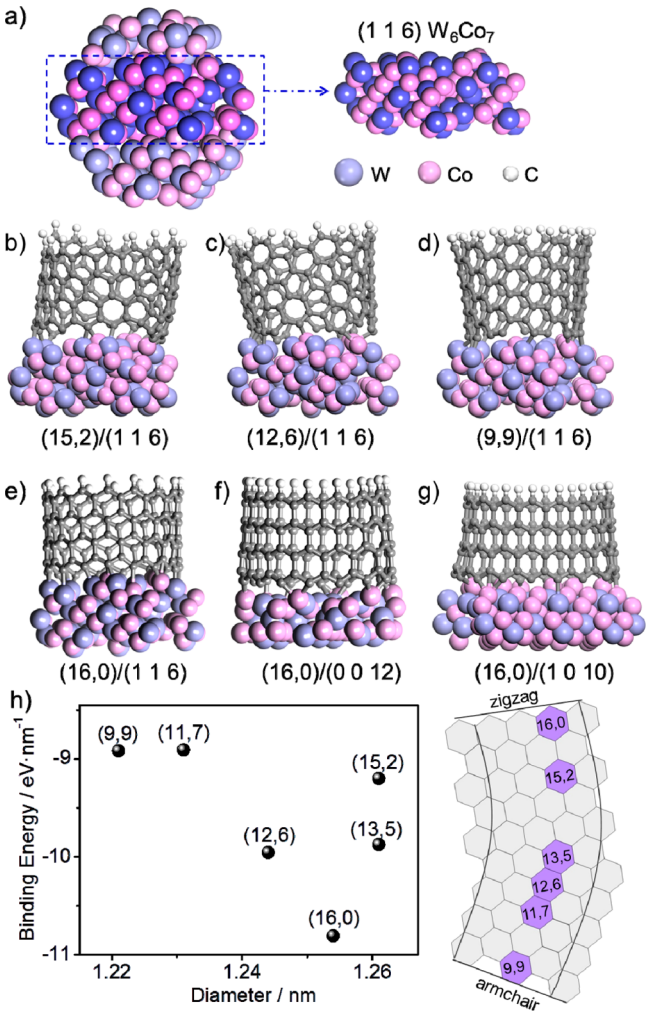

Figure 2. DFT simulation of SWNTs on W_6Co_7 nanocrystal. (a) Vertical view of (1 1 6) plane cut from a W_6Co_7 nanocrystal. (b–e) Side views of interfaces between the (1 1 6) plane of W_6Co_7 catalyst and SWNTs of different chiralities including (15,2) (e), (12,6) (f), (9,9) (g), and (16,0) (e), respectively. (f,g) Side views of interfaces between the (0 0 12) (f) and (1 0 10) (g) planes of W_6Co_7 catalyst and the (16,0) SWNT. (h) Binding energy of SWNTs with different chiralities on the (1 1 6) plane of W_6Co_7.

or more specifically binding energy of a SWNT on the W_6Co_7 nanoparticle, depends on its chirality rather than its diameter and that the (16,0) tube has the lowest binding energy. In addition, we also studied the structural match of a (16,0) SWNT with the different planes of W_6Co_7. It can be found that only (1 1 6) plane accords with the end structure of (16,0) SWNT (Figure 2e–g).

The simulation results indicate that (1 1 6) plane may act as the template to initiate the growth of (16,0) SWNTs.

Then we tried to promote the formation of (16,0) tubes by adjusting the chemical vapor deposition (CVD) conditions with the new W_6Co_7 catalysts. We found an optimized condition, i.e., 1050 °C, 150 $cm^3 \cdot min^{-1}$ H_2, and 200 $cm^3 \cdot min^{-1}$ Ar through the ethanol bubbler as carbon feeding stock, to produce SWNTs with radial breathing mode (RBM) peaks intensively concentrated at ~195 cm^{-1} (under excitations of both 532 and 785 nm) (Figure 3a). Much fewer RBMs can be detected with excitation

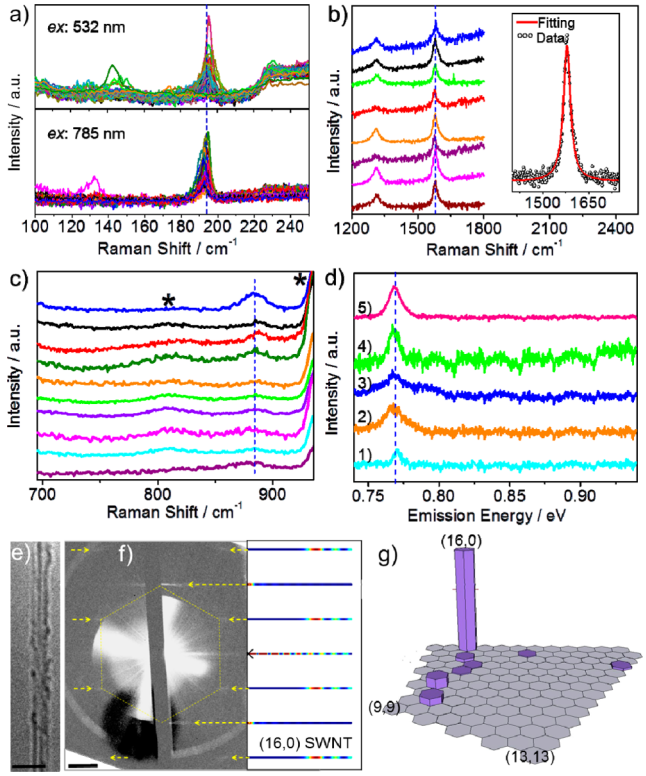

Figure 3. Characterizations of SWNTs grown at 1050 °C under the optimized conditions. (a) RBM-region Raman spectra taken with excitations of 532 and 785 nm. (b) G band Raman spectra, inset is the Lorenzian fitting of a G band (excitations: 532 and 785 nm). (c) The oTO-region Raman spectra (excitation: 785 nm). The bands indicated by * are Raman signals arising from the SiO_2/Si substrates. (d) Photoluminescence spectra taken with 785 nm (curve: 1–3) and 532 nm (curve: 4, 5) excitations. (e) HRTEM image of a SWNT bundle (scale bar: 10 nm). (f) Electron beam diffraction pattern of the tubes shown in (e) (scale bar: 2 nm^{-1}). The simulated (16,0) SWNT electron beam diffraction pattern is also shown. (g) Relative abundances of various chiralities quantified from 361 RBMs denoted in a partial SWNT chiral map.

wavelengths other than 532 and 785 nm (Figure S3). The corresponding tangential vibration (G mode) bands at ~1583 cm^{-1} exhibit single Lorentzian symmetric line shapes, which are typical features of semiconducting zigzag SWNTs (Figures 3b and S4).[32,33] The simultaneously observed broad bands assigned as Raman active feature related to the out-of-plane transverse optical (oTO) phonon branches all appear at the same wavenumbers (Figure 3c). The tube diameter (d_t) calculated from the ω_{RBM} with the equation reported in ref 31 is 1.25 nm. The chirality is assigned by comparing with the Kataura plot[34–36] to be (16,0) (Figure S5 and Table S1). The chirality assignment is verified by the photoluminescence spectroscopy.[37] The tubes

DOI: 10.1021/jacs.5b04403
J. Am. Chem. Soc. 2015, 137, 8688–8691

grown on the silicon sphere with RBMs at ~195 cm^{-1} exhibit fluorescence, indicating that these tubes are semiconductor. The fluorescence emission at ~0.77 eV with both 532 and 785 nm excitations (Figure 3d) corresponds to the first van Hove optical transition energy[38] (E_{11}) of (16,0) SWNT (Figure S6). To further confirm the chirality assignment unambiguously, we performed electron beam diffraction of the SWNTs. A bundle involved two SWNTs grown across the slits of silicon substrate with RBM frequency at ~195 cm^{-1} shows typical electron diffraction pattern indexed to (16,0) SWNT (Figures 3e,f, S7, and S8). The abundance of (16,0) SWNTs in the samples grown at 1050 °C under optimized CVD conditions are estimated from the micro-Raman spectra to be 79.2% (Figure 3g and Table S2). These results demonstrate the direct growth of zigzag (16,0) SWNTs in dominant abundance with the new W_6Co_7 catalyst.

According to the reported studies, growing zigzag SWNTs is very different from other types of SWNTs.[24,25] We designed the experiments to explore the growth behavior of (16,0) SWNTs. We performed the Raman mapping with 1 μm laser spot to estimate the (16,0) SWNT length. We found that 85.7% of (16,0) tubes have the length below 1 μm and only very few (16,0) tubes grow longer than 3 μm (Figure 4a). To further verify this

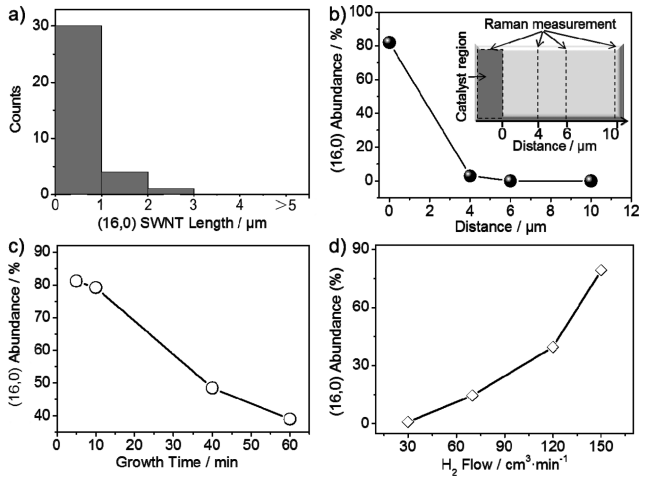

Figure 4. (a) Statistics for (16,0) SWNT length measured with Raman mapping (laser spot: 1 μm). (b) Selectivity of (16,0) SWNTs measured at different distances apart from the catalyst region. Inset shows the schematic of Raman mapping on different regions of silicon substrate. When performing Raman mapping on the catalyst region, we denote the distance as 0 μm. (c) Selectivity of (16,0) SWNTs at different growth time. (d) Selectivity of (16,0) SWNTs at different H_2 flow.

observation, we count the (16,0) SWNTs using Raman in regions with different distances away from the catalysts (Figure S9). At the catalyst region (the distance was denoted as 0 μm), the abundance of (16,0) SWNTs is 81.5%, which is the highest of all measured distances. Then the content of (16,0) tubes decreases apparently when counting the (16,0) tube at the distance of 4 μm away from the catalyst region (Figure 4b). These observations demonstrate that the (16,0) tubes nucleated on the catalyst nanoparticles are distinctly shorter than other (n,m) tubes. Prolonging the growth time also results in lower abundance of (16,0) tubes (Figure 4c and Table S4). These results all exhibit the unfavorable growth kinetics of zigzag (16,0) SWNTs, which has been predicted in theoretical simulations.[21−25]

We also used this new W_6Co_7 catalysts prepared at 1050 °C to catalyze SWNT growth with the exactly same CVD condition as that for (12,6) SWNT growth, i.e., 1030 °C, 30 $cm^3 \cdot min^{-1}$ H_2, and 200 $cm^3 \cdot min^{-1}$ Ar through the ethanol bubbler as carbon feeding stock. (12,6) SWNTs were still obtained at large proportion (Figure S10e). Besides, we also noticed a few of (16,0) SWNTs appeared (17 RBMs at ~195 cm^{-1} with both 532 and 785 nm excitations from 1750 measurements), which has never been observed in our (12,6)-enriched SWNT samples prepared under the exactly same condition reported in ref 31 (Figure S10). This indicates that the catalyst structure is important for the growth of SWNTs with specific chirality; however, the unfavorable growth kinetics is still an issue for the selective growth of (16,0) tubes. During the optimization of growth conditions, we found that the selectivity of (16,0) tubes is significantly improved by using a higher flow rate of H_2 (Figure 4d, Tables S2 and S3). It was reported that the hydrogen may lower the carbon fugacity on the catalyst surface and consequently delay the nucleation of the cap.[4] Therefore, increasing H_2 ratio in feed gas will suppress the growth of all types of tubes. Then the growth of the kinetically favorable nonzigzag SWNTs will be restrained more remarkably, and the inferiority in growing zigzag tubes will be effectively improved. The highly selective growth of (16,0) tubes can only be achieved when using the right catalysts together with proper growth conditions.

In conclusion, we have realized the selective growth of zigzag (16,0) SWNTs using W_6Co_7 catalysts. We believe that the structural match between the (16,0) tubes and the atomic arrangements of (1 1 6) planes of W_6Co_7 nanocrystals play an important role in the specified growth of (16,0) SWNTs. The structural match between the tubes and the catalyst nanocrystals presents the thermodynamic ascendancy for the chirality selective growth, but the growth kinetics is also crucial. By the cooperative function of the structural template effect of the catalyst nanocrystals and the optimization of growth kinetics, zigzag SWNTs can be dominantly produced. This should be a general strategy for the selective growth of zigzag (n,0) SWNTs and may also be helpful in the controlled preparation of other materials.

■ ASSOCIATED CONTENT

Supporting Information

Synthesis details, XRD, HRTEM measurements, DFT simulations, SEM, Raman and photoluminescence spectroscopy, and electron diffraction characterizations of the SWNTs. The Supporting Information is available free of charge on the ACS Publications website at DOI: 10.1021/jacs.5b04403.

■ AUTHOR INFORMATION

Corresponding Author

*yanli@pku.edu.cn

Notes

The authors declare the following competing financial interest(s): Y.L. and F.Y. declare a financial interest: patents related to this research have been filed by Peking University. The University's policy is to share financial rewards from the exploitation of patents with the inventors. The remaining authors declare no competing financial interests.

DOI: 10.1021/jacs.5b04403
J. Am. Chem. Soc. 2015, 137, 8688−8691

■ ACKNOWLEDGMENTS

We thank Prof. L. Qin, K. Liu, Dr. M. He, and J. Wei for discussions on electron diffraction, Dr. X. Li for TEM measurements, and Prof. K. Jiang for providing the Si_3N_4 specimens for TEM. This work is supported by Ministry of Science and Technology of China (Project 2011CB933003), the National Natural Science Foundation of China (projects 21125103, 91333105, and 21321001), and Beijing Municipal Science & Technology Commission (Project D141100000614001).

■ REFERENCES

(1) Iijima, S.; Ichihashi, T. *Nature* **1993**, *363*, 603.
(2) Bachilo, S. M.; Balzano, L.; Herrera, J. E.; Pompeo, F.; Resasco, D. E.; Weisman, R. B. *J. Am. Chem. Soc.* **2003**, *125*, 11186.
(3) Miyauchi, Y.; Chiashi, S.; Murakami, Y.; Hayashida, Y.; Maruyama, S. *Chem. Phys. Lett.* **2004**, *387*, 198.
(4) Lolli, G.; Zhang, L.; Balzano, L.; Sakulchaicharoen, N.; Tan, Y.; Resasco, D. E. *J. Phys. Chem. B* **2006**, *110*, 2108.
(5) Li, X.; Tu, X.; Zaric, S.; Welsher, K.; Seo, W. S.; Zhao, W.; Dai, H. *J. Am. Chem. Soc.* **2007**, *129*, 15770.
(6) Harutyunyan, A. R.; Chen, G.; Paronyan, T. M.; Pigos, E. M.; Kuznetsov, O. A.; Hewaparakrama, K.; Kim, S. M.; Zakharov, D.; Stach, E. A.; Sumanasekera, G. U. *Science* **2009**, *326*, 116.
(7) Chiang, W. H.; Sankaran, R. M. *Nat. Mater.* **2009**, *8*, 882.
(8) He, M.; Chernov, A. I.; Fedotov, P. V.; Obraztsova, E. D.; Sainio, J.; Rikkinen, E.; Jiang, H.; Zhu, Z.; Tian, Y.; Kauppinen, E. I. *J. Am. Chem. Soc.* **2010**, *132*, 13994.
(9) Wang, H.; Wang, B.; Quek, X. Y.; Wei, L.; Zhao, J.; Li, L. J.; Chan-Park, M. B.; Yang, Y.; Chen, Y. *J. Am. Chem. Soc.* **2010**, *132*, 16747.
(10) Liu, B.; Ren, W.; Li, S.; Liu, C.; Cheng, H.-M. *Chem. Commun.* **2012**, *48*, 2409.
(11) He, M.; Jiang, H.; Liu, B.; Fedotov, P. V.; Chernov, A. I.; Obraztsova, E. D.; Cavalca, F.; Wagner, J. B.; Hansen, T. W.; Anoshkin, I. V.; Obraztsova, E. A.; Belkin, A. V.; Sairanen, E.; Nasibulin, A. G.; Lehtonen, J.; Kauppinen, E. I. *Sci. Rep.* **2013**, *3*, 1460.
(12) Chen, Y.; Shen, Z.; Xu, Z.; Hu, Y.; Xu, H.; Wang, S.; Guo, X.; Zhang, Y.; Peng, L.; Ding, F.; Liu, Z.; Zhang, J. *Nat. Commun.* **2013**, *4*, 2205.
(13) Wang, H.; Yuan, Y.; Wei, L.; Goh, K.; Yu, D. S.; Chen, Y. *Carbon* **2015**, *81*, 1.
(14) Page, A. J.; Ding, F.; Irle, S.; Morokuma, K. *Rep. Prog. Phys.* **2015**, *78*, 036501.
(15) Avouris, P.; Chen, Z.; Perebeinos, V. *Nat. Nanotechnol.* **2007**, *2*, 605.
(16) Shulaker, M. M.; Hills, G.; Patil, N.; Wei, H.; Chen, H.-Y.; Wong, H. S. P.; Mitra, S. *Nature* **2013**, *501*, 526.
(17) De Volder, M. F. L.; Tawfick, S. H.; Baughman, R. H.; Hart, A. J. *Science* **2013**, *339*, 535.
(18) Jain, R. M.; Howden, R.; Tvrdy, K.; Shimizu, S.; Hilmer, A. J.; McNicholas, T. P.; Gleason, K. K.; Strano, M. S. *Adv. Mater.* **2012**, *24*, 4436.
(19) Rao, R.; Liptak, D.; Cherukuri, T.; Yakobson, B. I.; Maruyama, B. *Nat. Mater.* **2012**, *11*, 213.
(20) Liu, B.; Liu, J.; Tu, X.; Zhang, J.; Zheng, M.; Zhou, C. *Nano Lett.* **2013**, *13*, 4416.
(21) Ding, F.; Harutyunyan, A. R.; Yakobson, B. I. *Proc. Natl. Acad. Sci. U. S. A.* **2009**, *106*, 2506.
(22) Dumlich, H.; Reich, S. *Phys. Rev. B: Condens. Matter Mater. Phys.* **2010**, *82*, 085421.
(23) Li, H.-B.; Page, A. J.; Irle, S.; Morokuma, K. *J. Am. Chem. Soc.* **2012**, *134*, 15887.
(24) Artyukhov, V. I.; Penev, E. S.; Yakobson, B. I. *Nat. Commun.* **2014**, *5*, 4892.
(25) Yuan, Q.; Ding, F. *Angew. Chem., Int. Ed.* **2015**, *54*, 5924.
(26) Fouquet, M.; Bayer, B. C.; Esconjauregui, S.; Thomsen, C.; Hofmann, S.; Robertson, J. *J. Phys. Chem. C* **2014**, *118*, 5773.
(27) Liu, J.; Wang, C.; Tu, X.; Liu, B.; Chen, L.; Zheng, M.; Zhou, C. *Nat. Commun.* **2012**, *3*, 1199.
(28) Sanchez-Valencia, J. R.; Dienel, T.; Gröning, O.; Shorubalko, I.; Mueller, A.; Jansen, M.; Amsharov, K.; Ruffieux, P.; Fasel, R. *Nature* **2014**, *512*, 61.
(29) Reich, S.; Li, L.; Robertson, J. *Chem. Phys. Lett.* **2006**, *421*, 469.
(30) Dutta, D.; Chiang, W.-H.; Sankaran, R. M.; Bhethanabotla, V. R. *Carbon* **2012**, *50*, 3766.
(31) Yang, F.; Wang, X.; Zhang, D.; Yang, J.; Da, L.; Xu, Z.; Wei, J.; Wang, J.-Q.; Xu, Z.; Peng, F.; Li, X.; Li, R.; Li, Y.; Li, M.; Bai, X.; Ding, F.; Li, Y. *Nature* **2014**, *510*, 522.
(32) Saito, R.; Jorio, A.; Hafner, J.; Lieber, C.; Hunter, M.; McClure, T.; Dresselhaus, G.; Dresselhaus, M. *Phys. Rev. B: Condens. Matter Mater. Phys.* **2001**, *64*, 085312.
(33) Michel, T.; Paillet, M.; Nakabayashi, D.; Picher, M.; Jourdain, V.; Meyer, J. C.; Zahab, A. A.; Sauvajol, J. L. *Phys. Rev. B: Condens. Matter Mater. Phys.* **2009**, *80*, 245416.
(34) Dresselhaus, M. S.; Dresselhaus, G.; Saito, R.; Jorio, A. *Phys. Rep.* **2005**, *409*, 47.
(35) Soares, J. S.; Cançado, L. G.; Barros, E. B.; Jorio, A. *Phys. Status Solidi B* **2010**, *247*, 2835.
(36) Zhang, D.; Yang, J.; Yang, F.; Li, R.; Li, M.; Ji, D.; Li, Y. *Nanoscale* **2015**, *7*, 10719.
(37) Bachilo, S. M.; Strano, M. S.; Kittrell, C.; Hauge, R. H.; Smalley, R. E.; Weisman, R. B. *Science* **2002**, *298*, 2361.
(38) Liu, K.; Deslippe, J.; Xiao, F.; Capaz, R. B.; Hong, X.; Aloni, S.; Zettl, A.; Wang, W.; Bai, X.; Louie, S. G. *Nat. Nanotechnol.* **2012**, *7*, 325.

DOI: 10.1021/jacs.5b04403
J. Am. Chem. Soc. 2015, 137, 8688−8691